Effects of gravity and nonlinearity on the waves in the granular chain

Jongbae Hong and Aiguo Xu
Department of Physics and Center for Strongly Correlated Materials Research, Seoul National University, Seoul 151-742, Korea
(Received 20 January 2001; published 24 May 2001)

The solitary signal observed in a horizontal granular chain changes its speed and form due to gravity in a vertical chain. We find that all the propagating signals in a vertical chain follow power laws in depth for propagating speed, grain velocity, amplitude, and width. This stems from the power-law type changing of elastic properties in a medium under gravity. The propagation may be separated into two types according to the behavior of the power-law exponents, depending on the strength of the nonlinearity. We show that the power-law exponents are constants in the strength of the impulse in the weakly nonlinear regime, while they depend on the strength of the impulse in the strongly nonlinear regime. We derive power-law exponents for the weakly nonlinear regime analytically and try to understand the behaviors of the strongly nonlinear regime through analytical treatment.

DOI: 10.1103/PhysRevE.63.061310 PACS number(s): 45.70.−n, 46.40.Cd, 02.70.Ns, 43.25.+y

I. INTRODUCTION

Granular media are ubiquitous around us. Therefore, understanding their properties will be very useful in many areas of industrial applications [1,2]. One useful property is the nature of propagation, reflection, and transmittion of waves in a granular medium [3–7]. From this one may get information about the interior of the granular medium. A granular medium is a unique state of matter, because it is neither the usual liquid nor the usual solid [8]. The solid state of the granular medium has very complicated force chains inside it [8], along which elastic signals propagate easily. The contact force between grains is nonlinear and usually of the power-law type [4].

Even though force chains in a granular medium are not simple, we study in this work a simplified one-dimensional model composed of equal masses coupled by a nonlinear power-law type contact force. Spherical and ellipsoidal grains give rise to a Hertz type contact force represented by $F \propto \delta^{3/2}$, where F is the squeezing force and δ is the squeezed distance between grains. The Hertzian contact force for spherical or ellipsoidal linear media can be obtained analytically [9]. The geometrical nature of the contacting area is solely responsible for the exponent 3/2. Sands, soils, and other irregular particulate media have a power-law contact force of exponent 2 [4]. Bead or sphere assemblages also have a exponent 2 for a certain pressure range [4]. Since the contact force determines the dynamics of the granular system, it is probably meaningful to study the granular chain with arbitrary power-law exponent of the contact force for application to real irregular grains. A different situation of the granular chain has been studied recently [10].

The horizontal granular chain with Hertzian contact has been studied by Nesterenko [3] who showed that the propagating mode in a highly nonlinear regime is a soliton of a different kind from the one given by the Korteweg–de Vries equation [11]. Nesterenko obtained a particlelike equation of motion in the highly nonlinear regime, i.e., under strong impulse. Recently, MacKay [12] has proved the existence of a solitary wave in the horizontal Hertzian chain using a rather general mathematical theorem given by Friesecke and Wattis [13]. Ji and Hong [14] have extended MacKay's proof to the case of arbitrary power-law exponent. A numerical study of the arbitrary power-law exponent has been done by Manciu *et al.* [15] Experimental verification of the soliton in the horizontal Hertzian chain has been provided using a series of steel balls [16,17]. The effect of loading on the solitary wave [18] and interesting properties of soliton crossings [19] have been studied recently.

Sometimes a granular medium is placed under a constant force field, e.g., gravity. A constant electric (magnetic) field may exert a constant force on charged (magnetized) grains. The discrete medium becomes denser as we go along the direction of the applied field, and the propagating properties of elastic waves, such as speed, width, etc., may change along the direction of the applied force, since the elastic properties of the medium change due to the applied force. The propagation and backscattering behavior of solitary waves in the Hertzian chain has been studied intensively and extensively [20]. These works, including Ref. [7], suggested a possible way to detect a buried material inside a granular medium using elastic impulse. But more work is needed for practical purposes.

The objective of this work is to study the effect of gravity and the effect of nonlinearity on signal propagation in the vertical nonlinear granular chain. Molecular dynamics simulation clearly shows that gravity causes decreasing amplitude, slowing down of grain oscillation, and dispersion of signal width as the signal goes down the chain. All these behaviors follow certain power laws, which originate from the power-law type contact force and gravity. Our previous work [21] presented a mathematical analysis for those behaviors due to gravity in the weakly nonlinear regime. But the analysis was incomplete. This work presents a corrected derivation for the power-law exponents when the impulse is weak. Molecular dynamics simulation also shows that the power-law exponents depend on the strength of nonlinearity when the impulse is strong, while they are independent of the strength of nonlinearity when the impulse is weak. This will be discussed analytically.

This paper is composed as follows. We first present in Sec. II molecular dynamics simulation results ranging from weak to strong impulse. A weak impulse gives rise to a weakly nonlinear oscillatory signal and a strong impulse

gives rise to a rather solitary signal. Characteristics of both oscillatory and solitary signals show power-law behaviors in depth as they propagate down. Various power-law exponents obtained by simulation are given. In Sec. III, we analyze the propagation nature of the wave in the weakly nonlinear regime. The power-law behaviors in this region can be explained by a linear dispersive wave equation obtained as a limit of the weak impulse, which maps the vertical granular chain onto a horizontal granular chain with varying force constant. Section IV attempts an analytical understanding of the signal behaviors in the strongly nonlinear regime. We explain the role of nonlinearity in this regime. We present conclusions in Sec. V.

II. SIMULATION

We focus on the motion of grains in a vertical granular chain with a power-law type nonlinear contact force of arbitrary exponent. Since it is usually hard to treat nonlinear problems analytically, we first present the results of molecular dynamics simulations for the equation of motion of grains under consideration in this work. The equation of motion of a grain at a vertical position z_i, which is the distance from the top of the vertical chain to the center of ith grain, is written as

$$m\ddot{z}_n = \eta[\{\Delta_0-(z_n-z_{n-1})\}^p-\{\Delta_0-(z_{n+1}-z_n)\}^p]+mg, \tag{1}$$

where m is the mass of the grain, Δ_0 is the distance between centers of the adjacent grains, p is the exponent of the power-law contact force, and η is the elastic constant of the grain under consideration. Therefore, the overlap between adjacent grains at the nth contact is $\delta_n=\Delta_0-(z_{n+1}-z_n)$. We do not consider plastic deformation in treating Eq. (1). For the Hertzian chain, i.e., $p=3/2$, the equation of motion comes from the Hertzian interaction energy between neighboring grains, which is given by [9]

$$V(\delta_n)=\frac{2}{5D}\left(\frac{R_nR_{n+1}}{R_n+R_{n+1}}\right)^{1/2}\delta_n^{5/2}\equiv b\,\delta_n^{5/2}, \tag{2}$$

where R_n is the radius of the spherical grain and

$$D=\frac{3}{4}\left(\frac{1-\sigma_n^2}{E_n}+\frac{1-\sigma_{n+1}^2}{E_{n+1}}\right), \tag{3}$$

where σ_n,σ_{n+1} and E_n,E_{n+1} are Poisson's ratios and Young's moduli of the bodies at neighboring positions, respectively [9]. Therefore, $\eta=\frac{5}{2}b$ for the Hertzian chain.

To perform numerical simulations for Eq. (1), we choose a vertical chain of N grains, where N ranges between 1000 and 5000 according to our need. We choose 10^{-5} m, 2.36×10^{-5} kg, and 1.0102×10^{-3} s as the units of distance, mass, and time, respectively. These units give the gravitational acceleration $g=1$ [7]. We set the grain diameter to 100, mass to 1, and the constant η of Eq. (1) to 5657 for molecular dynamics simulation. The equilibrium condition

$$mgn=\eta\delta_n^p \tag{4}$$

has been used for the nth contact of the vertical chain. Using the third-order Gear predictor-corrector algorithm [22] as a calculational tool, we perform numerical simulations for arbitrary p including $p=3/2$. We choose various strengths of impulse for our study. For this purpose we neglect plastic deformation [17,23] and viscoelastic dissipation in our model system.

Figure 1 shows snapshots of three typical types of grain velocity signal propagating down the vertical chain of Hertzian contact. Figure 1(a), which is obtained for the initial impulse velocity $v_i=0.001$ in our program units, shows typical grain velocity signals appearing in the weakly nonlinear regime, Fig. 1(b) obtained for $v_i=1$ is the signal of the intermediate regime, and Fig. 1(c) for $v_i=1000$ shows the characteristics of the strongly nonlinear regime in which the tail disappears. The common features of the propagation characteristics shown in Fig. 1 are increasing signal speed, decreasing grain velocity, and increasing signal width as the signal goes down. The straight lines drawn on a log-log scale in Fig. 2 certify that the depth-dependent behaviors of the leading and second-leading peaks of grain velocity and displacement are all of power-law type. According to our numerical fits shown in Fig. 2, the explicit expressions for the depth-dependent behaviors of the leading amplitudes of grain displacement and velocity are given by $A_{max}(h)\propto h^{-0.0835\pm0.0003}$ and $v_{max}(h)\propto h^{-0.2500\pm0.0001}$ for $v_i=0.001$ and $p=3/2$. We obtain other depth-dependent power laws showing the dispersiveness of the signal. One of them is the number of particles participating in the leading part of velocity signal, $N(h)$, which describes the length scale of the signal. The other is the elapsed time to reach maximum amplitude $T_{max}(h)$, which describes the time scale of the signal. The power-law behaviors of these quantities with error bounds are $\lambda\propto N\propto h^{0.338\pm0.004}$ and $T_{max}\propto h^{0.170\pm0.002}$. These numerical data well satisfy the relations of an oscillating signal, such as $T=A/v$ and $\lambda=Tv_p$, where v_p is the phase velocity of the signal, even though the oscillation is not perfectly periodic. The phase velocity $v_p\propto h^{1/6}$ is the well-known phase velocity of the signal propagating down a medium with Hertzian contact [4,5].

We also obtain power-law exponents of the leading grain velocity and signal speed v_p for a wide range of impulse strength from $v_i=10^{-3}$ to $v_i=10^3$ for $p=1.2,1.5$, and 2.0 in Fig. 3. The logarithmic scale has been used only for the abscissa of the graph in Fig. 3. Both Fig. 3(a) and Fig. 3(b) have similar structures. One can see a trend that as v_i decreases to less than 0.1 the exponents approach saturated values for a given p, and the exponents vanish when v_i is larger than 10^3. A transition region exists between $v_i=0.1$ and $v_i=10^3$. These features are common to any value of $p>1$.

A remarkable feature shown in Fig. 3 is that there is a region in which the characteristics of signal propagation are independent of the strength of impulse v_i for any $p>1$. We called this region the weakly nonlinear regime where the signal is oscillatory. A typical form of the signal in this regime was shown in Fig. 1(a). The power-law behaviors of the signal in the flat region of Fig. 3 are explained analytically in the next section using the linear dispersive wave

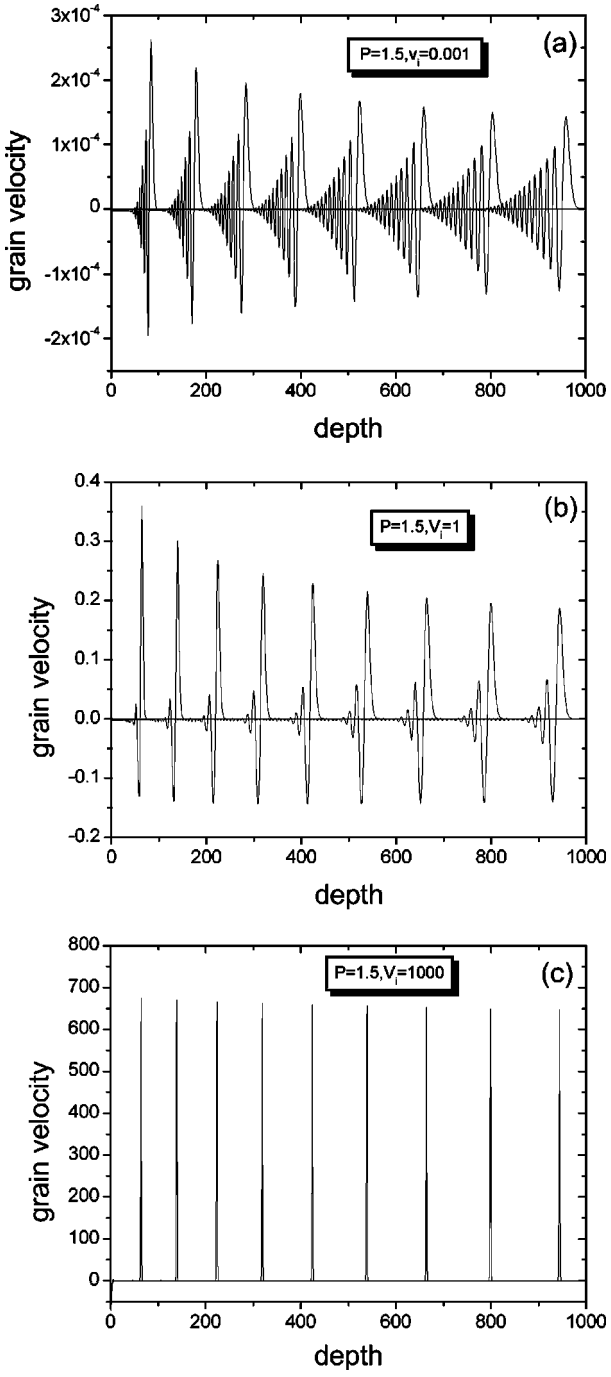

FIG. 1. Snapshots of typical modes of propagating signals under weak, intermediate, and strong impulses in the vertical granular chain with Hertzian contact. (a) Oscillatory mode due to weak impulse $v_i=0.001$. (b) Quasisolitary mode due to intermediate impulse $v_i=1$. (c) Quasisolitary mode due to strong impulse $v_i=1000$.

equation as a limiting case of weak nonlinearity. Another region in which the exponent changes rather rapidly may be called the strongly nonlinear regime where the signal is rather solitary as shown in Fig. 1(c). There is an intermediate regime where a weak oscillatory part remains in the tail of the signal as shown in Fig. 1(b). The signal in the intermediate regime is a combination of a nonlinear solitary and a linear oscillatory wave.

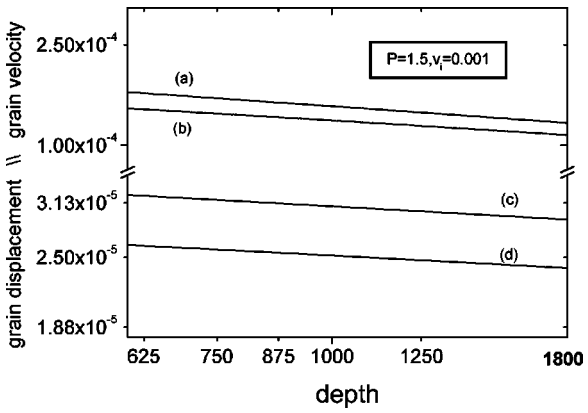

FIG. 2. Upper part shows the plots of leading (a) and second-leading (b) peaks of grain velocity versus depth drawn in log-log scale. Lower part shows the plots of leading (c) and second-leading (d) peaks of displacement versus depth drawn in log-log scale. $p=3/2$. $v_i=0.001$.

In the limit of strong impulse, gravity is negligible; therefore the system is nothing more than the horizontal chain in which a complete soliton is created [3,12,14]. In the region

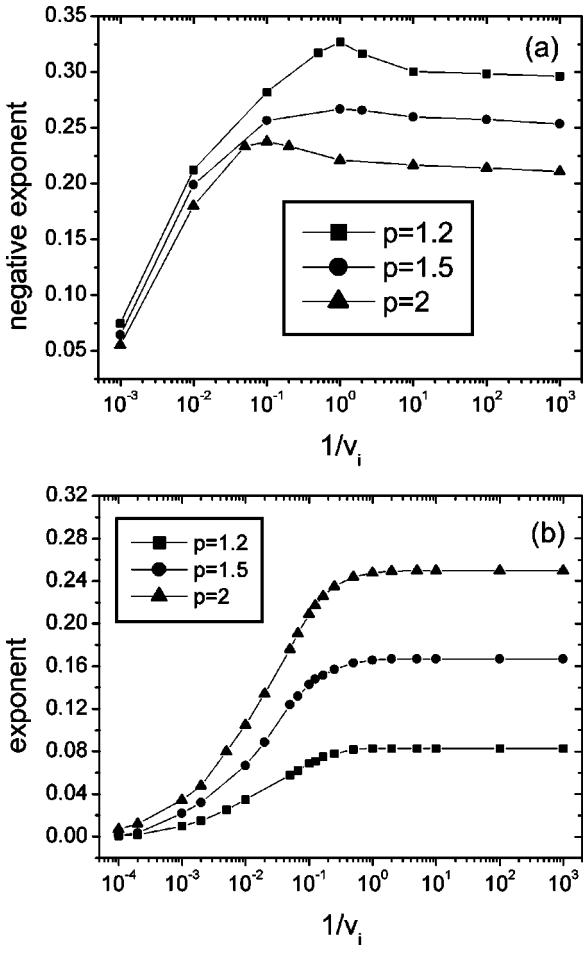

FIG. 3. Plots of power-law exponents of leading grain velocity (a) and signal speed (b) versus v_i for several p's. Logarithmic-scale has been applied only to abscissa.

of moderately strong impulse, however, the gravity effect is not negligible, and it causes a change in the elastic properties of the medium as depth increases. Thus the height, the width, and the speed of the soliton change, because the medium changes. Therefore, the system under strong impulse is mostly dominated by the nonlinearity of the system. We discuss this matter in Sec. IV.

III. WEAKLY NONLINEAR REGIME

An interesting phenomenon we discovered above is that the absolute value of the power-law exponent of grain velocity and signal speed increases and approaches a saturated value for a given contact force as the strength of the initial impulse decreases. This was shown in Fig. 3. The propagating mode in this saturated region, which corresponds to the weakly nonlinear regime, is oscillatory. The oscillation amplitude, frequency, and wavelength follow power laws. These interesting behaviors of the signal in this regime may be described by a linear dispersive wave equation if we go to the limit of the weakly nonlinear region.

We rederive various power-law exponents, since some errors were involved in the process of derivation in our previous work [21]. For this purpose, we introduce a new variable ψ_n, denoting the displacement of the nth grain from equilibrium, defined by

$$\psi_n = z_n - n\Delta_0 + \sum_{l=1}^{n} \left(\frac{mgl}{\eta}\right)^{1/p}, \tag{5}$$

where the last term is the sum of grain overlaps up to the nth contact and we set $z_0=\psi_0=0$. Equation (1) is transformed into

$$m\ddot{\psi}_n = \eta\left[\left(\frac{mgn}{\eta}\right)^{1/p} + (\psi_{n-1}-\psi_n)\right]^p - \eta\left[\left\{\frac{mg(n+1)}{\eta}\right\}^{1/p} + (\psi_n-\psi_{n+1})\right]^p + mg \tag{6}$$

using Eq. (5).

For the weakly nonlinear regime, the condition

$$|\psi_{n-1}-\psi_n| \ll \left(\frac{mgn}{\eta}\right)^{1/p} \tag{7}$$

is valid and the expansion of Eq. (6) under this condition reads

$$m\ddot{\psi}_n = -\mu_n(\psi_n-\psi_{n-1}) + \mu_{n+1}(\psi_{n+1}-\psi_n) \tag{8}$$

where $\mu_n = mpg(\eta/mg)^{1/p} n^{1-1/p}$ is the force constant of the nth contact of the linear horizontal chain. We drop weak nonlinear terms of the expansion in Eq. (8) to make the system linear. Thus the vertical granular chain becomes a horizontal chain with varying force constants in which the gravity effect is contained. Both the left and right sides of Eq. (8) are linear in ψ_n. Therefore, the scaling analysis tells us that the equation of motion (8) has nothing to do with the initial impulse v_i.

To analyze this linear difference equation analytically, we reexpress Eq. (8) in the continuum limit, i.e.,

$$\rho\frac{\partial^2}{\partial t^2}\psi(h,t) = \frac{\partial}{\partial h}\left[\tau(h)\frac{\partial}{\partial h}\psi(h,t)\right] \tag{9}$$

when the intergrain distance $\Delta_0 \to 0$, where $\tau(h) = \tau_1(h/\Delta_0)^{1-1/p}$ denotes the depth-dependent tension, and $\rho = m/\Delta_0$ and $\tau_1 = \mu_1\Delta_0$ are the density and the tension of the chain at the first contact, respectively. We set $c_1 = \sqrt{\tau_1/\rho}$, which is the well-known speed of a wave in a string of tension τ_1 and density ρ.

Since Eq. (9) is a linear differential equation, we can apply Fourier analysis to this equation. Then we have the following dispersion relation for the complex wave number $k(\omega) = k_r + ik_i$:

$$\omega(k) = k_r\sqrt{\frac{\tau(h)}{\rho}}\left[1+\frac{\tau'^2}{4\tau^2k_r^2}\right]^{1/2} \tag{10}$$

and $k_i = -\tau'/2\tau$. From Eq. (10), we obtain the phase and group velocity as follows:

$$v_p = \frac{\omega}{k} \approx \sqrt{\frac{\tau(h)}{\rho}}\left[1+\frac{\tau'^2}{8\tau^2k_r^2}\right] \tag{11}$$

and

$$v_g = \frac{d\omega}{dk} \approx \sqrt{\frac{\tau(h)}{\rho}}\left[1-\frac{\tau'^2}{8\tau^2k_r^2}\right]. \tag{12}$$

Here and in what follows k means k_r. The difference between v_p and v_g denotes that the wave is dispersive, and $k_i \neq 0$ normally means the wave is diffusive [24].

Treating dispersive and diffusive waves is not simple. However, since $\tau'/\tau \propto h^{-1}$ and therefore e^{-k_ih} is constant in h, the envelope function of the wave is not exponentially damping, so it is not diffusive for this special case. Therefore, the general solution of the linear equation (9) is written as

$$\psi(h,t) = \sum_{\omega} A(\omega)e^{i(kh-\omega t)} \tag{13}$$

and the h dependence of the envelope of the function $\psi(h,t)$ is solely given by the coefficient $A(\omega)$. Now we solve Eq. (9) again using $\psi_\zeta(h,t) = u_\zeta(h)e^{i\zeta t}$ as a normal mode solution, where $u_\zeta(h) = A(\omega)e^{ikh}$ and $\omega \propto \zeta$. Then $u_\zeta(h)$ satisfies

$$\frac{d^2}{dh^2}u_\zeta(h) + \frac{1-1/p}{h}\frac{d}{dh}u_\zeta(h) + \frac{\zeta^2}{h^{1-1/p}}u_\zeta(h) = 0, \tag{14}$$

which is a type of Bessel differential equation [25]. A solution of this equation propagating to the positive h direction is given by the Hankel function [25]

$$u_\zeta(h) = h^\xi H_\nu^{(1)}(\theta h^\gamma), \tag{15}$$

where $\xi=1/2p, \gamma=\frac{1}{2}+\xi=\frac{1}{2}(1+1/p), \theta=\zeta/\gamma$, and $\nu=\xi/\gamma=1/(1+p)$.

The asymptotic form of Eq. (15) at large h for a fixed ν is

$$u_\zeta(h)\approx\sqrt{\frac{2}{\pi\theta}}h^{\xi-\gamma/2}e^{i[\theta h^\gamma-(\pi/2)\nu-\pi/4]} \tag{16}$$

and the displacement is written as

$$\psi_\zeta(h,t)\approx h^{\xi-\gamma/2}e^{i[(\zeta/\gamma)h^\gamma-\zeta t]}. \tag{17}$$

Therefore, the depth dependence of the coefficient $A(\omega)$ of the displacement signal is

$$A(\omega(h))=h^{\xi-\gamma/2}=h^{-(1-1/p)/4} \tag{18}$$

for all ω.

To obtain other depth-dependent properties of the signal, we need more information about the signal. This is given by an asymptotic analysis for the linear wave equation. The asymptotic form of the solution of the general linear equation is given by the saddle-point method or the steepest descent method. The result is written as [25]

$$\psi(h,t)\cong\frac{\sqrt{2\pi}A(\omega_s)\exp[i\{k_sh-\omega(k_s)t\}-\alpha]}{\{t|\omega''(k_s)|\}^{1/2}} \tag{19}$$

when $\omega''(k)\neq 0$, where k_s means the wave number at the saddle point, and $\alpha=(i\pi/4)\mathrm{sgn}\omega''(k_s)$. When there are many saddle points, the asymptotic solution must be the sum over all saddle points. This work concerns the case of a single saddle point; therefore the amplitude of the general solution of the linear wave equation in the asymptotic regime is given by $A(\omega_s)\{t|\omega''(k_s)|\}^{-1/2}$ where $t=h/v_g$. Since we showed that $A(\omega_s)$ exhausts the depth dependence of the amplitude of displacement $\psi(h,t)$, $\{t|\omega''(k_s)|\}^{1/2}$ must be depth independent. This condition gives information about the wave number k. Differentiating Eq. (12) once more, we get information on k,

$$t|\omega''(k_s)|\propto\frac{h\tau'^2}{\tau^2}k^{-3}\propto h^0. \tag{20}$$

This relation provides one piece of key information

$$k\propto h^{-1/3} \tag{21}$$

in obtaining the power-law behavior of the signal.

We already obtained the power-law behaviors in depth for the amplitude of displacement (18) and the wave number (21). With this information and the signal velocity $v_p\propto h^{(1-1/p)/2}$ from Eq. (11), we obtain the depth-dependent behavior of the grain velocity and its oscillation frequency using the relation for a linear wave $\omega(h)=k(h)v_p(h)$, and the relation for an oscillating signal $1/\omega(h)\propto A(h)/v(h)$. They are given by

$$v(h)\propto h^{-(1/3+1/p)/4}, \tag{22}$$

$$\omega(h)\propto h^{1/6-1/2p}. \tag{23}$$

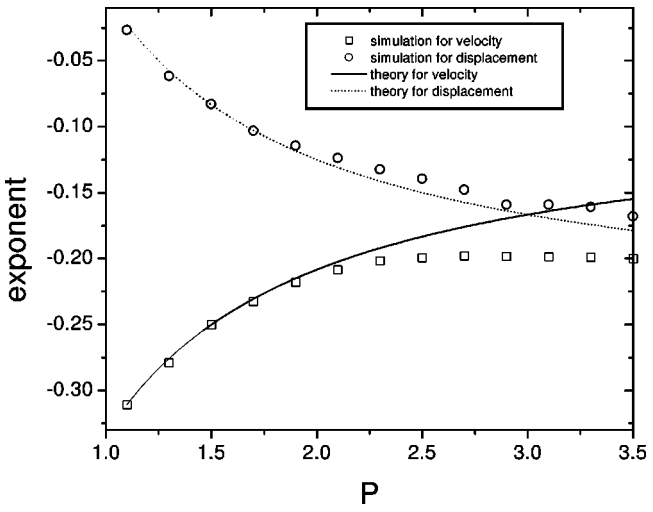

FIG. 4. Dependence of power-law exponents of grain velocity and displacement on the exponent of the contact force p. Numerical data are compared with theoretical prediction. Solid lines are theoretical results. Circles and squares denote simulation data for displacement and grain velocity, respectively. Data are obtained for the leading peaks of each signal.

The characteristic time of oscillation which is expressed by the period is given by the inverse of the frequency or the ratio of displacement to grain velocity, i.e.,

$$T(h)=\frac{A(h)}{v(h)}\propto\omega(h)^{-1}\propto h^{-1/6+1/2p}. \tag{24}$$

The characteristic length of oscillation, on the other hand, which is expressed by the wavelength is given by multiplying $T(h)$ by the phase velocity, i.e.,

$$\lambda(h)=T(h)v_p(h)\propto h^{1/3}. \tag{25}$$

The depth-dependent power-law behaviors obtained numerically for the weakly nonlinear regime in the last section agree quite well with Eqs. (22)–(25) obtained analytically. This analysis explains the damping and dispersive behavior due to gravity for the weakly nonlinear regime in a vertical granular chain. To check the theoretical prediction given above, we obtain peak values of the displacement and grain velocity signal for other values of p and compare them with theory in Fig. 4. One can see very nice fits to the theoretical curves. For large values of p, a deviation from theory occurs, especially in grain velocity. This is understandable because the nonlinearity becomes stronger as p increases and the grain velocity contains more derivatives than the displacement. Interestingly enough, however, the characteristic length of the signal does not depend on p.

IV. STRONGLY NONLINEAR REGIME

In Sec. III, we explained the power-law behavior of signal propagation under gravity only for the weakly nonlinear regime shown by simulation in Sec. II. Figure 3 shows power-law exponents of grain velocity and signal speed versus the initial impulse v_i which is a measure of nonlinearity of the

system. The flat region of Fig. 3 named the weakly nonlinear regime was discussed in Sec. III. We will discuss the v_i-dependent region, named the strongly nonlinear regime, in this section.

In strongly nonlinear regime it is rather difficult to analyze the simulation result analytically. But one may understand the effect of gravity, which causes a power-law increase of signal speed and width and decrease of signal height, through a rather simple analysis. For this purpose, we perform a similar transformation to the one above for the analysis of the weakly nonlinear regime.

For the strongly nonlinear regime, the condition

$$(\psi_{n-1}-\psi_n) \gg \left(\frac{mgn}{\eta}\right)^{1/p} \tag{26}$$

is valid and expansion under this condition leads Eq. (6) to

$$\begin{aligned} m\ddot{\psi}_n = {} & \eta[(\psi_{n-1}-\psi_n)^p + pg_n(\psi_{n-1}-\psi_n)^{p-1}] \\ & - \eta[(\psi_n-\psi_{n+1})^p + pg_{n+1}(\psi_n-\psi_{n+1})^{p-1}] \end{aligned} \tag{27}$$

where $g_n=(mgn/\eta)^{1/p}$ denotes grain overlap at the nth contact. The gravity term can be neglected in the highly nonlinear regime, since the gravity effect appears in the coefficient g_n. The different orders of ψ_n in the left and right sides of Eq. (27) imply that v_i dependence must appear in the signal characteristics.

If we set $A_{n+1}=(\psi_n-\psi_{n+1})^p$ and $A_n=(\psi_{n-1}-\psi_n)^p$ and use the relations

$$\frac{\partial A_{n+1}}{\partial \psi_{n+1}} = -p(\psi_n-\psi_{n+1})^{p-1},$$

$$\frac{\partial A_n}{\partial \psi_n} = -p(\psi_{n-1}-\psi_n)^{p-1},$$

Eq. (27) is written as

$$m\ddot{\psi}_n = -\eta(A_{n+1}-A_n) + \eta\left[g_{n+1}\frac{\partial A_{n+1}}{\partial \psi_{n+1}} - g_n\frac{\partial A_n}{\partial \psi_n}\right]. \tag{28}$$

This equation is rewritten in a continuum form,

$$\begin{aligned} \rho\ddot{\psi}(h) &= -\eta\frac{\partial A}{\partial h} + \eta\frac{\partial}{\partial h}\left[g(h)\frac{\partial A}{\partial \psi}\right] \\ &= -\eta\left[1-\frac{\partial}{\partial h}\left(g(h)\frac{\partial h}{\partial \psi}\right)\right]\frac{\partial A}{\partial h} \qquad (29) \\ &\quad + \eta\left[g(h)\frac{\partial h}{\partial \psi}\right]\frac{\partial^2 A}{\partial h^2}. \qquad (30) \end{aligned}$$

The first term on the right-hand side of Eq. (29) is just the one describing a perfect soliton in the horizontal chain [3] and the second term is responsible for the changing speed, height, and width of signal due to gravity as signal goes down. We separate dispersion part out in the expression Eq. (30), in which damping and dispersion of a soliton are dominated by the gravity factor $g(h)$ and the nonlinearity factor $\partial h/\partial \psi$. The latter is rewritten as $(\partial h/\partial t)(\partial t/\partial \psi)$ which is equivalent to v_p/v_i or v_p/v_{grain} by dimensional analysis. Therefore, the signal characteristics approach the soliton created in the horizontal chain as nonlinearity, i.e., v_i, increases in the strongly nonlinear regime. One can see this behavior in Fig. 3.

The role of each term of Eq. (30) cannot be superposed independently, since the equation is nonlinear. Therefore, a fully analytical treatment of Eq. (30) is not simple. The nonlinear regime, therefore, requires more work to understand the phenomenon fully. We just showed that the force exerted in the equation of motion for the strongly nonlinear regime can be divided into a nongravity part and a gravity part as shown in Eq. (29), and also divided into a damping part and a dispersion part as shown in Eq. (30). Therefore, one may understand that a soliton created by the nongravity force $-\eta\partial A/\partial h$ of Eq. (29) changes its speed, height, and width under gravity coupled with nonlinearity. Figures 1(a), 1(b), and 1(c) show the change of signal as v_i increases explicitly.

All characteristics of the signal follow power laws in depth and the absolute values of the power-law exponents decrease as v_i increases. This was shown in Fig. 3.

V. CONCLUSION

We saw in Sec. II that the depth-dependent power-law behavior of the propagating signal in a gravitationally compacted granular chain is generic for the whole range of strength of impulse or nonlinearity. For a rather weak impulse regime, which we call the weakly nonlinear regime, the power-law exponent of the grain velocity approaches a saturated value, i.e., it does not depend on the strength of the nonlinearity for a given contact force. The signal in this region is oscillatory. Comprehensive study of this region is one of the main subjects of this work. The equation of motion of the displacement of a grain in the limit of weak nonlinearity can be transformed into a linear differential equation where Fourier analysis is applicable. The asymptotic behavior of the linear differential equation is given by the saddle-point method. This provides independent information for the wave number of the signal. Normal mode analysis combined with this information gives rise to all other information for signal propagation depending on depth in the asymptotic regime. Characteristics of the linear dispersive signal are applicable for understanding the signal behavior yielded in the weakly nonlinear regime. The exponents given by analytic study agree well with simulation data.

For the strongly nonlinear regime in which impulse is strong, simulation shows that the power-law exponents depend on the strength of impulse v_i, in other words, the strength of nonlinearity of the system. The signal becomes more solitary as the impulse increases. But this quasisolitary signal changes its speed, damps, and disperses due to gravity as it goes down the chain. The behaviors of the signal, such as grain velocity and amplitude, signal speed, and width, also follow power laws in depth. The absolute value of the expo-

nents of the power-law behaviors approaches zero as the impulse becomes stronger. This implies that the role of gravity becomes negligible as the impulse increases. One can understand this phenomenon from Eq. (30), showing that the gravity factor is always coupled with the nonlinearity factor, which is inversely proportional to the impulse v_i. This tells us that increasing nonlinearity diminishes the gravity effect. Therefore, the signal under very strong impulse is similar to that of the horizontal chain in which a nondispersing soliton is the propagating mode [3,12].

We separated the force exerted on a grain under strong impulse into three in Eq. (30). One may guess the role of each term from its form and may understand conceptually the power-law behaviors and v_i dependence in the strongly nonlinear regime as shown numerically in Sec. II. But the three forces cannot be combined linearly in describing a quasisolitary signal. Further work is needed to fully understand the signal behaviors in the rather strongly nonlinear regime.

The equation of motion for the weakly nonlinear regime is equivalent to those of a nonuniform transmission line and a nonuniform string. Therefore, one may apply the analysis of this work to other areas. The behavior of the soliton under gravity or other constant force field may be applicable in the applied sciences.

ACKNOWLEDGMENTS

This work was supported by Korea Research Foundation Grant No. KRF-2000-DP0106 and the Brain Korea 21 Project.

[1] *Physics of Dry Granular Media*, edited by H. J. Herrmann, J.-P. Hovi, and S. Luding (Kluwer Academic Publishers, Dordrecht, 1998).
[2] *Powders and Grains 97*, edited by R. P. Behringer and J. T. Jenkins (A. A. Balkema, Rotterdam, 1997).
[3] V. F. Nesterenko, J. Appl. Mech. Tech. Phys. **5**, 733 (1983); V. F. Nesterenko, J. Phys. IV **55**, C8-729 (1994).
[4] J.D. Goddard, Proc. R. Soc. London, Ser. A **430**, 105 (1990).
[5] R. S. Sinkovits and S. Sen, Phys. Rev. Lett. **74**, 2686 (1995).
[6] S. Sen and R. S. Sinkovits, Phys. Rev. E **54**, 6857 (1996).
[7] S. Sen, M. Manciu, and J. D. Wright, Phys. Rev. E **57**, 2386 (1998).
[8] H. M. Jaeger and S. R. Nagel, Science **255**, 1523 (1995); H. M. Jaeger, S. R. Nagel, and R. P. Behringer, Rev. Mod. Phys. **68**, 1259 (1996).
[9] L. D. Landau and E. M. Lifshitz, *Theory of Elasticity* (Pergamon, Oxford, 1970).
[10] E. Hascoët, H. J. Herrmann, and V. Loreto, Phys. Rev. E **59**, 3202 (1999).
[11] R. M. Miura, SIAM Rev. **18**, 412 (1976).
[12] R. S. MacKay, Phys. Lett. A **251**, 8589 (1999).
[13] G. Friesecke and J. A. D. Wattis, Commun. Math. Phys. **161**, 391 (1994).
[14] J.-Y. Ji and J. Hong, Phys. Lett. A **260**, 60 (1999).
[15] M. Manciu, V. Tehan, and S. Sen, Physica A **268**, 644 (1999).
[16] A. N. Lazaridi, and V. F. Nesterenko, J. Appl. Mech. Tech. Phys. **26**, 405 (1985).
[17] C. Coste, E. Falcon, and S. Fauve, Phys. Rev. E **56**, 6104 (1997).
[18] M. Manciu, V. Tehan, and S. Sen, Chaos **10**, 658 (2000).
[19] M. Manciu, S. Sen, and A. J. Hurd, Phys. Rev. E **63**, 016614 (2001).
[20] M. Manciu, S. Sen, and A. J. Hurd, Physica A **274**, 588 (1999); **274**, 607 (1999).
[21] J. Hong, J.-Y. Ji, and H. Kim, Phys. Rev. Lett. **82**, 3058 (1999).
[22] M. P. Allen and D. J. Tildesley, *Computer Simulation of Liquids* (Clarendon, Oxford, 1987).
[23] K. L. Johnson, *Contact Mechanics* (Cambridge University Press, Cambridge, 1992).
[24] P. L. Bhatnagar, *Nonlinear Waves in One-Dimensional Dispersive Systems* (Clarendon, Oxford, 1979).
[25] *Handbook of Mathematical Functions*, edited by M. Abramowitz and I. A. Stegun, Natl. Bur. of Stand. Appl. Math. Ser. No. 55 (U.S. GPO, Washington, DC, 1972).